

VU Research Portal

Energy Densities in the Strong-Interaction Limit of Density Functional Theory

Mirtschink, A.; Seidl, M.; Gori Giorgi, P.

published in

Journal of Chemical Theory and Computation
2012

DOI (link to publisher)

[10.1021/ct3003892](https://doi.org/10.1021/ct3003892)

document version

Publisher's PDF, also known as Version of record

[Link to publication in VU Research Portal](#)

citation for published version (APA)

Mirtschink, A., Seidl, M., & Gori Giorgi, P. (2012). Energy Densities in the Strong-Interaction Limit of Density Functional Theory. *Journal of Chemical Theory and Computation*, 8, 3097-3107.
<https://doi.org/10.1021/ct3003892>

General rights

Copyright and moral rights for the publications made accessible in the public portal are retained by the authors and/or other copyright owners and it is a condition of accessing publications that users recognise and abide by the legal requirements associated with these rights.

- Users may download and print one copy of any publication from the public portal for the purpose of private study or research.
- You may not further distribute the material or use it for any profit-making activity or commercial gain
- You may freely distribute the URL identifying the publication in the public portal ?

Take down policy

If you believe that this document breaches copyright please contact us providing details, and we will remove access to the work immediately and investigate your claim.

E-mail address:

vuresearchportal.ub@vu.nl

Energy Densities in the Strong-Interaction Limit of Density Functional Theory

André Mirtschink,[†] Michael Seidl,[‡] and Paola Gori-Giorgi^{†,*}

[†]Department of Theoretical Chemistry and Amsterdam Center for Multiscale Modeling, FEW, Vrije Universiteit, De Boelelaan 1083, 1081HV Amsterdam, The Netherlands

[‡]Institute of Theoretical Physics, University of Regensburg, D-93040 Regensburg, Germany

ABSTRACT: We discuss energy densities in the strong-interaction limit of density functional theory, deriving an exact expression within the definition (gauge) of the electrostatic potential of the exchange-correlation hole. Exact results for small atoms and small model quantum dots (Hooke's atoms) are compared with available approximations defined in the same gauge. The idea of a local interpolation along the adiabatic connection is discussed, comparing the energy densities of the Kohn–Sham, the physical, and the strong-interacting systems. We also use our results to analyze the local version of the Lieb–Oxford bound, widely used in the construction of approximate exchange-correlation functionals.

1. INTRODUCTION

Increasing the accuracy of the approximations to the exchange-correlation energy functional $E_{xc}[\rho]$ of Kohn–Sham (KS) density functional theory (DFT) is of crucial importance for research areas ranging from theoretical chemistry and biochemistry to solid-state and surface physics (for a recent review, see, e.g., ref 1).

A piece of *exact* information on $E_{xc}[\rho]$ is provided by the strong-interaction limit of DFT, in which the coupling constant of the electron–electron interaction becomes infinitely large while the one-electron density $\rho(\mathbf{r})$ does not change.^{2–5} This defines a fictitious system with the same density as the physical one and maximum possible correlation between the relative electronic positions, useful to describe situations in which restricted Kohn–Sham DFT encounters problems, such as low-density many-particle scenarios and the breaking of the chemical bond.^{6,7} The exact mathematical structure of this limit has been uncovered only recently,^{8–10} and exact calculations (at least for simple systems) have started to become available.^{6,7,11}

The aim of this paper is to make a step forward in the inclusion of this new piece of exact information into approximations to the exchange-correlation energy functional $E_{xc}[\rho]$. Previous attempts in this direction^{3–5} focused on global (i.e., integrated over all space) quantities, introducing size-consistency errors. The exact solution of the strong-interaction limit, now available, makes accessible not only global but also *local* quantities, from which it is easier to construct size-consistent approximations^{12–14} (for a critical review on size consistency of approximate energy density functionals, see, e.g., ref 15 and, especially, ref 16).

Local quantities are in general not uniquely defined (see, e.g., ref 17 for further discussion on the exchange-correlation energy density and refs 18–21 for the kinetic energy density), and we have to be specific on their definition (also called *gauge*). Here, we focus on the conventional, physically transparent, definition in terms of the electrostatic energy of the exchange-correlation hole. We derive the exact expression within this definition in

the strong-interaction limit, and we evaluate it for small atoms and small model quantum dots, making comparisons with available approximations within the same gauge. We then discuss the idea of a local interpolation along the adiabatic connection by comparing energy densities in the physical case, the weak- and the strong-interaction limit.

As a byproduct, our results allow us to analyze the local version of the Lieb–Oxford bound, a condition widely used to construct approximate exchange-correlation functionals. It is well-known that the Lieb–Oxford bound is an exact condition^{22–24} on the global $E_{xc}[\rho]$. Many nonempirical approximate functionals, however, use its local version, which is a sufficient but not necessary condition to ensure the global bound (see, e.g., refs 25, 26, and 27). Our analysis strongly suggests that the local version of the Lieb–Oxford bound is formulated in the gauge of the electrostatic potential of the exchange-correlation hole. This, in turn, implies that the local bound is certainly violated at least in the tail region of a molecular or atomic density, and in the bond region of a stretched molecule.

The paper is organized as follows. In section 2, we review the DFT adiabatic connection as a tool to build approximate $E_{xc}[\rho]$, highlighting the role of the strong-interaction limit and discussing the size-consistency problem of interpolations based on global quantities. In section 3, we discuss energy densities in general, and we introduce the gauge of the electrostatic energy associated with the exchange-correlation hole. The exact expression for this quantity in the strong-interaction limit is derived in section 4, where approximations are also discussed. In particular, we analyze the “point-charge plus continuum” (PC) model functional,⁴ showing that it is an approximation to the energy density within the same conventional definition considered here. Energy densities along the adiabatic connection are discussed and analyzed in section 5. We then use our results to discuss the local version of the Lieb–Oxford

Received: May 16, 2012

Published: July 17, 2012



bound in section 6. The last section, section 7, is devoted to conclusions and perspectives. Finally, a simple illustration for the case of the uniform electron gas is reported in the Appendix.

2. INTERPOLATION ALONG THE ADIABATIC CONNECTION

Within the framework of the adiabatic connection,^{28–30} the exchange-correlation energy can be expressed by the coupling constant integration

$$E_{xc}[\rho] = \int_0^1 d\lambda \langle \Psi_\lambda[\rho] | \hat{V}_{ee} | \Psi_\lambda[\rho] \rangle - U[\rho] \\ \equiv \int_0^1 d\lambda W_\lambda[\rho] \quad (1)$$

with $\Psi_\lambda[\rho]$ being the ground state wave function of a fictitious system with scaled electron–electron interaction

$$\hat{H} = \hat{T} + \lambda \hat{V}_{ee} + \hat{V}_{ext}^\lambda \quad (2)$$

The external potential \hat{V}_{ext}^λ is adjusted to keep the density $\rho_\lambda(\mathbf{r})$ associated with $\Psi_\lambda[\rho]$ in agreement with the physical density, $\rho_\lambda(\mathbf{r}) = \rho_1(\mathbf{r}) \equiv \rho(\mathbf{r})$. For the weak interaction limit ($\lambda = 0$), we encounter the Kohn–Sham³¹ reference system, and the integrand $W_0[\rho]$ becomes the exact exchange energy $E_x[\rho]$. For the strong-interaction limit ($\lambda \rightarrow \infty$), a reference system within the strictly correlated electrons concept (SCE)^{2,3,8,9} can be defined. The asymptotic expansions of $W_\lambda[\rho]$ are

$$W_{\lambda \rightarrow 0}[\rho] = E_x[\rho] + 2\lambda E_c^{GL2}[\rho] + O(\lambda^2) \quad (3)$$

$$W_{\lambda \rightarrow \infty}[\rho] = W_\infty[\rho] + \frac{W'_\infty[\rho]}{\sqrt{\lambda}} + O(\lambda^{-p}) \quad (4)$$

where $E_c^{GL2}[\rho]$ is the correlation energy given by second order Görling–Levy perturbation theory (GL2)³² and $p \geq 5/4$.⁹ Exact expressions for the functionals $W_\infty[\rho]$ and $W'_\infty[\rho]$ are given, respectively, in refs 8 and 9.

Expression 1 for the exchange-correlation energy is exact as long as the exact dependence of the integrand on λ is known.^{33,34} As this is obviously not the case, eq 1 still enables approximate exchange-correlation energies by modeling $W_\lambda[\rho]$ along the adiabatic connection.

Attempts toward approximate $W_\lambda[\rho]$ were initiated by Becke,³⁵ introducing the half and half functional, in which a model is defined assuming a linear dependence of $W_\lambda[\rho]$ on λ and setting $W_0[\rho]$ equal to exact exchange and $W_1[\rho]$ to LSDA exchange-correlation. This results in a functional with 50% exact exchange and 50% LSDA exchange-correlation. Further adjustment of the portion of exact exchange by semiempirical arguments gives rise to hybrid functionals like B3LYP.^{36–39} The adiabatic connection may also be used for the construction of nonempirical hybrids as in ref 40, where a model for $W_\lambda[\rho]$ consisting of two intersected straight lines fixed by exact exchange, GGA exchange, and GGA exchange-correlation is defined. Ernzerhof⁴¹ introduced a curved model by proposing a Padé interpolation for the integrand using as input exact exchange and $E_c^{GL2}[\rho]$ in the weak interaction limit and GGA exchange-correlation for $\lambda = 1$.

The models we have mentioned so far for the integrand (except for B3LYP) share in common that for the weak interaction limit, exact exchange is employed, and for the physical situation with $\lambda = 1$, information from approximate

DFT (DFA) is used. The argument for the recourse to exact exchange is that DFA exchange works well only if combined with DFA correlation. This is due to error cancellation. Consequently, DFA exchange-correlation can be used for the physical case where exchange and correlation are employed together. As error cancellation in DFA exchange-correlation might not be satisfactory, a continuation of the ansatz of Ernzerhof⁴¹ is possible by taking DFA exchange-correlation at some intermediate λ instead of $\lambda = 1$. This would allow one to balance the exchange error with the correlation error. Along this line, Mori-Sánchez et al.⁴² constructed their MCY1 functional: a Padé interpolation is undertaken with exact exchange and meta-GGA exchange input in the weak interaction limit and meta-GGA exchange-correlation for an intermediate λ (chosen semiempirically).

The discussed models clearly outperform the stand alone DFAs upon which they are based.^{35,40–42} Nonetheless, employment of DFA quantities in their construction can lead to serious misbehavior in the curvature of the integrand as demonstrated by Peach et al.⁴³ by comparison of the MCY1 approximation with accurate quantities along the adiabatic connection (see, e.g., Figure 3 in ref 43). In the same paper, the authors show that accurate exchange-correlation energy can be recovered via an interpolation with accurate full-CI ingredients.

A model that could avoid unfavorable DFA bias is the interaction strength interpolation (ISI).^{2–4,9} Here, exact information from the weak interaction limit is employed, namely exact exchange and GL2, together with information from the strong interaction limit. The λ dependence of $W_\lambda[\rho]$ is then modeled by an interpolation between the two limits. As at the time of emergence of the ISI exact quantities for the strong interaction limit were not available, the point-charge plus continuum (PC) model was introduced.^{2–4} The PC model provides approximate expressions for $W_\infty[\rho]$ and $W'_\infty[\rho]$ in a DFA spirit and, consequently, can lead to erroneous behavior of $W_\lambda[\rho]$ (see below for more discussion). A full avoidance of DFA bias is possible within the SCE many-electron formalism, within which the functionals $W_\infty[\rho]$ and $W'_\infty[\rho]$ can be accurately computed.^{8,9} Refs 8 and 9 compare the PC solutions with the exact SCE values for small atoms: while $W_\infty^{PC}[\rho]$ is a very reasonable approximation to its exact counterpart,⁸ the original $W_\infty^{PC}[\rho]$ turned out to be much less accurate.⁹ The exact results could be used to propose a revised PC approximation $W_\infty^{revPC}[\rho]$ having accuracy similar to that of $W_\infty^{PC}[\rho]$. Further comparison is undertaken in section 4.2 of this paper for a more subtle quantity, the local energy density that will be defined in the next sections.

Although free of any DFA bias (if we use exact input quantities), an unpleasant feature of the ISI is the violation of size consistency. This is due to the nonlinear way the (size-consistent) ingredients $W_0[\rho]$, $W'_0[\rho]$, $W_\infty[\rho]$, and $W'_\infty[\rho]$ enter the interpolation. For example, the revised ISI (which behaves better in the $\lambda \rightarrow \infty$ limit than the original ISI) reads⁹

$$W_\lambda^{revISI}[\rho] = \frac{\partial}{\partial \lambda} \left(a[\rho]\lambda + \frac{b[\rho]\lambda}{\sqrt{1 + c[\rho]\lambda + d[\rho]}} \right) \quad (5)$$

where a , b , c , and d are nonlinear functions of $W_0[\rho]$, $W'_0[\rho]$, $W_\infty[\rho]$, and $W'_\infty[\rho]$, determined by imposing the asymptotic expansions of eqs 3 and 4:

$$a[\rho] = W_\infty[\rho] \quad (6)$$

$$b[\rho] = -\frac{8E_c^{\text{GL}2}[\rho] W_\infty'[\rho]^2}{(E_x[\rho] - W_\infty[\rho])^2} \quad (7)$$

$$c[\rho] = \frac{16E_c^{\text{GL}2}[\rho]^2 W_\infty'[\rho]^2}{(E_x[\rho] - W_\infty[\rho])^4} \quad (8)$$

$$d[\rho] = -1 - \frac{8E_c^{\text{GL}2}[\rho] W_\infty'[\rho]^2}{(E_x[\rho] - W_\infty[\rho])^3} \quad (9)$$

Notice that the lack of size consistency is shared by all functionals in which the exact exchange energy (or any global energy) enters in a nonlinear way, thus, also, for example, MCY1.

As a final remark on the revISI functional, we can add that if one makes the approximation $E_c^{\text{GL}2} \approx E_c^{\text{MP}2}$, it can be viewed as a double hybrid functional (see, e.g., refs 44–47). With respect to available double hybrids, the revISI lacks size consistency, but it has the advantage of being able to deal with the small-gap systems problematic for perturbation theory. The practical impact of the lack of size consistency of the revISI functional in this context still needs to be tested, but from theoretical grounds it can be expected that difficulties in dissociating chemical bonds might arise (for further discussion in the context of fractional electron numbers, see, e.g., refs 48–51).

3. ENERGY DENSITIES: DEFINITIONS

A possible way to recover size consistency in the ISI framework is to use a *local* integrand in eq 1:

$$E_{\text{xc}}[\rho] = \int_0^1 d\lambda \int d\mathbf{r} \rho(\mathbf{r}) w_\lambda[\rho](\mathbf{r}) \quad (10)$$

The idea is then to build a local model, $w_\lambda^{\text{ISI}}[\rho](\mathbf{r})$, by interpolating between the $\lambda \rightarrow 0$ and the $\lambda \rightarrow \infty$ limits. As anticipated in section 1, the energy density $w_\lambda[\rho](\mathbf{r})$ is not uniquely defined, and an important requirement to construct an interpolation is that the input local quantities in the weak- and in the strong-interaction limits are defined in a consistent manner (same gauge).

One of the most widely used definitions of the energy density in DFT is in terms of the exchange-correlation hole (see, e.g., refs 12, 13, and 14) $h_{\text{xc}}^\lambda(\mathbf{r}, \mathbf{r}')$:

$$w_\lambda[\rho](\mathbf{r}) = \frac{1}{2} \int \frac{h_{\text{xc}}^\lambda(\mathbf{r}, \mathbf{r}')}{|\mathbf{r} - \mathbf{r}'|} d\mathbf{r}' \quad (11)$$

where

$$h_{\text{xc}}^\lambda(\mathbf{r}, \mathbf{r}') = \frac{P_2^\lambda(\mathbf{r}, \mathbf{r}')}{\rho(\mathbf{r})} - \rho(\mathbf{r}') \quad (12)$$

and the pair-density $P_2^\lambda(\mathbf{r}, \mathbf{r}')$ is obtained from the wave function $\Psi_\lambda[\rho]$ of eqs 1 and 2:

$$P_2^\lambda(\mathbf{r}, \mathbf{r}') = N(N-1) \times \sum_{\sigma_1 \dots \sigma_N} |\Psi_\lambda(\mathbf{r}\sigma_1, \mathbf{r}'\sigma_2, \mathbf{r}_3\sigma_3, \dots, \mathbf{r}_N\sigma_N)|^2 d\mathbf{r}_3 \dots d\mathbf{r}_N \quad (13)$$

In the definition of eq 11, $w_\lambda[\rho](\mathbf{r})$ is the electrostatic potential of the exchange-correlation hole (a negative charge distribution normalized to -1), around a reference electron in \mathbf{r} . This quantity at the physical coupling strength $\lambda = 1$ (plus the Hartree potential) has also been called $v_{\text{cond}}(\mathbf{r})$ in the literature (see, e.g., ref 52).

The energy density $w_\lambda[\rho](\mathbf{r})$ in the $\lambda \rightarrow \infty$ limit in the gauge of eq 11 is the central quantity of this paper: in the next section, we will derive an exact expression using the strictly correlated electron concept, and we will evaluate it for small atoms and quantum dots (Hooke's atoms). Notice that the relevance of $w_\infty[\rho](\mathbf{r})$ for the construction of a new generation of approximate $E_{\text{xc}}[\rho]$ has also been pointed out very recently by Becke.⁵³

4. ENERGY DENSITIES IN THE STRONG INTERACTION LIMIT

4.1. Exact. When $\lambda \rightarrow \infty$, the wave function $\Psi_\lambda[\rho]$ tends to the strictly correlated electron state, $\Psi_{\lambda \rightarrow \infty}[\rho] \rightarrow \Psi_{\text{SCE}}[\rho]$, with^{8,9}

$$|\Psi_{\text{SCE}}(\mathbf{r}_1, \dots, \mathbf{r}_N)|^2 = \frac{1}{N!} \sum_{\mathcal{P}} \int d\mathbf{s} \frac{\rho(\mathbf{s})}{N} \delta(\mathbf{r}_1 - \mathbf{f}_{\mathcal{P}(1)}(\mathbf{s})) \times \delta(\mathbf{r}_2 - \mathbf{f}_{\mathcal{P}(2)}(\mathbf{s})) \dots \delta(\mathbf{r}_N - \mathbf{f}_{\mathcal{P}(N)}(\mathbf{s})) \quad (14)$$

where $\mathbf{f}_1, \dots, \mathbf{f}_N$ are “co-motion functions”, with $\mathbf{f}_i(\mathbf{r}) \equiv \mathbf{r}$, and \mathcal{P} denotes a permutation of $\{1, \dots, N\}$. This means that the N points $\mathbf{r}_1, \dots, \mathbf{r}_N$ in 3D space found upon simultaneous measurement of the N electronic positions in the SCE state always obey the $N-1$ relations

$$\mathbf{r}_i = \mathbf{f}_i(\mathbf{r}_1) \quad (i = 2, \dots, N) \quad (15)$$

In other words, the position of one electron determines all the relative $N-1$ electronic positions (the limit of *strict correlation*). All the $N-1$ co-motion functions $\mathbf{f}_i(\mathbf{s})$ satisfy the differential equation

$$\rho(\mathbf{f}_i(\mathbf{r})) d\mathbf{f}_i(\mathbf{r}) = \rho(\mathbf{r}) d\mathbf{r} \quad (16)$$

which, together with the group properties^{8,10} of $\mathbf{f}_i(\mathbf{r})$, ensure that the SCE wave function of eq 14 yields the given density $\rho(\mathbf{r})$. Equation 16 has a simple physical interpretation: since the position of one electron determines the position of all the others, the probability of finding one electron in the volume element $d\mathbf{r}$ about \mathbf{r} must be the same of finding the i th electron in the volume element $d\mathbf{f}_i(\mathbf{r})$ about $\mathbf{f}_i(\mathbf{r})$.

Inserting eq 14 into eq 13, we obtain for the pair density $P_2^{\lambda \rightarrow \infty}(\mathbf{r}_1, \mathbf{r}_2) = P_2^{\text{SCE}}(\mathbf{r}_1, \mathbf{r}_2)$ in the strong-interaction limit

$$P_2^{\text{SCE}}(\mathbf{r}_1, \mathbf{r}_2) = \sum_{\substack{i,j=1 \\ i \neq j}}^N \int d\mathbf{s} \frac{\rho(\mathbf{s})}{N} \delta(\mathbf{r}_1 - \mathbf{f}_i(\mathbf{s})) \delta(\mathbf{r}_2 - \mathbf{f}_j(\mathbf{s})) \quad (17)$$

which also has a transparent physical meaning: two electrons can only be found at strictly correlated relative positions.

We first compute

$$\int \frac{P_2^{\text{SCE}}(\mathbf{r}, \mathbf{r}')}{|\mathbf{r} - \mathbf{r}'|} d\mathbf{r}' = \sum_{\substack{i,j=1 \\ i \neq j}}^N \int d\mathbf{s} \frac{\rho(\mathbf{s})}{N} \frac{\delta(\mathbf{r} - \mathbf{f}_i(\mathbf{s}))}{|\mathbf{r} - \mathbf{f}_j(\mathbf{s})|} \quad (18)$$

where, on the right-hand side, we have already integrated over the variable \mathbf{r}' . From the properties of the Dirac δ distribution and of the co-motion functions, eq 18 becomes

$$\int \frac{P_2^{\text{SCE}}(\mathbf{r}, \mathbf{r}')}{|\mathbf{r} - \mathbf{r}'|} d\mathbf{r}' = \frac{1}{N} \sum_{i,j=1}^N \frac{\rho(\mathbf{f}_i^{-1}(\mathbf{r})) |\det \partial_{\alpha} \mathbf{f}_{i,\beta}^{-1}(\mathbf{r})|}{|\mathbf{r} - \mathbf{f}_j(\mathbf{f}_i^{-1}(\mathbf{r}))|}$$

$$= \frac{\rho(\mathbf{r})}{N} \sum_{i,j=1}^N \frac{1}{|\mathbf{r} - \mathbf{f}_j(\mathbf{f}_i^{-1}(\mathbf{r}))|} \quad (19)$$

where $|\det \partial_{\alpha} \mathbf{f}_{i,\beta}^{-1}(\mathbf{r})|$ (with $\alpha, \beta = x, y, z$) is the determinant of the Jacobian of the transformation $\mathbf{r} \rightarrow \mathbf{f}_i^{-1}(\mathbf{r})$, and we have used the fact that all of the $\mathbf{f}_i(\mathbf{r})$ (and their inverses, which, by virtue of the group properties of the co-motion functions are also co-motion functions for the same configuration^{8,9}) satisfy eq 16. Now, we can use once more the group properties of the co-motion functions to recognize that for all $i \neq j$ the function $\mathbf{f}_j(\mathbf{f}_i^{-1}(\mathbf{r}))$ must be another co-motion function with the exclusion of $\mathbf{f}_i(\mathbf{r}) = \mathbf{r}$ (the identity can arise only if $i = j$). The double sum in the last term of eq 19 is then exactly equal to N times a single sum over all of the co-motion functions $\mathbf{f}_k(\mathbf{r})$ with $k \geq 2$, so that

$$\int \frac{P_2^{\text{SCE}}(\mathbf{r}, \mathbf{r}')}{|\mathbf{r} - \mathbf{r}'|} d\mathbf{r}' = \rho(\mathbf{r}) \sum_{k=2}^N \frac{1}{|\mathbf{r} - \mathbf{f}_k(\mathbf{r})|} \quad (20)$$

Inserting eq 20 into eqs 11 and 12, we finally obtain

$$w_{\infty}(\mathbf{r}) = \frac{1}{2} \sum_{k=2}^N \frac{1}{|\mathbf{r} - \mathbf{f}_k(\mathbf{r})|} - \frac{1}{2} v_{\text{H}}(\mathbf{r}) \quad (21)$$

where $v_{\text{H}}(\mathbf{r})$ is the Hartree potential. Notice that in previous work the exact $W_{\infty}[\rho]$ was given as^{7–9}

$$W_{\infty}[\rho] = \frac{1}{2} \int d\mathbf{r} \frac{\rho(\mathbf{r})}{N} \sum_{i,j=1}^N \frac{1}{|\mathbf{f}_i(\mathbf{r}) - \mathbf{f}_j(\mathbf{r})|} - U[\rho] \quad (22)$$

suggesting a corresponding energy density

$$\tilde{w}_{\infty}(\mathbf{r}) = \frac{1}{N} \sum_{i=1}^N \left(\frac{1}{2} \sum_{j=1, j \neq i}^N \frac{1}{|\mathbf{f}_i(\mathbf{r}) - \mathbf{f}_j(\mathbf{r})|} - \frac{1}{2} v_{\text{H}}(\mathbf{f}_i(\mathbf{r})) \right) \quad (23)$$

Equations 23 and 21 yield the same $W_{\infty}[\rho]$ when integrated with the density $\rho(\mathbf{r})$ but are locally different. They show a general feature of the co-motion functions: any given energy density $w_{\infty}^a(\mathbf{r})$ can always be transformed into a different energy density $w_{\infty}^b(\mathbf{r})$ defined as

$$w_{\infty}^b(\mathbf{r}) \equiv \frac{1}{N} \sum_{i=1}^N w_{\infty}^a(\mathbf{f}_i(\mathbf{r})) \quad (24)$$

When multiplied by the density $\rho(\mathbf{r})$, $w_{\infty}^a(\mathbf{r})$ and $w_{\infty}^b(\mathbf{r})$ integrate to the same quantity, because all of the co-motion functions (and their inverses, which are also co-motion functions) satisfy eq 16. Only eq 21 corresponds to the gauge of the exchange-correlation hole defined by eqs 11–13.

4.2. Approximations: The PC Model. The point-charge-plus-continuum (PC) model^{4,54} is a physically sound approximation to the $\lambda \rightarrow \infty$ indirect electron–electron repulsion energy $W_{\infty}[\rho]$. The idea is to rewrite the indirect Coulomb interaction energy $W_{\lambda}[\rho]$ as the electrostatic energy $E_{\text{es}}[\Psi_{\lambda}, \rho]$ of a system of N electrons in the state $\Psi_{\lambda}[\rho]$

embedded in a smeared background of positive charge $\rho_+(\mathbf{r}) = \rho(\mathbf{r})$.⁴ In fact, this total electrostatic energy $E_{\text{es}}[\Psi_{\lambda}, \rho]$ is just the sum of the electron–electron repulsion energy, $E_{\text{ee}} = \langle \Psi_{\lambda} | \hat{V}_{\text{ee}} | \Psi_{\lambda} \rangle$, the electron–background attraction energy, $E_{\text{eb}} = -2U[\rho]$, and the background–background repulsion energy $E_{\text{bb}} = U[\rho]$, thus yielding exactly $E_{\text{es}}[\Psi_{\lambda}, \rho] = E_{\text{ee}} + E_{\text{eb}} + E_{\text{bb}} = W_{\lambda}[\rho]$.

This relation is valid for every λ , but in the $\lambda \rightarrow \infty$ limit, when $\Psi_{\lambda} \rightarrow \Psi_{\text{SCE}}$, we expect that the electrons minimize $E_{\text{es}}[\Psi_{\lambda}, \rho]$ by occupying relative positions that divide the space into neutral cells with possibly zero (or weak) lowest-order electrostatic multipole moments.⁴ The idea is then that for one of the SCE configurations $\{\mathbf{r}_1, \mathbf{r}_2, \dots, \mathbf{r}_N\}$ we may approximate the indirect electron–electron repulsion by the sum of the electrostatic energies of all of the cells (i.e., we neglect the cell–cell interaction in view of their neutrality and low multipole moments):

$$\varepsilon_{\text{es}}(\mathbf{r}, \mathbf{f}_2(\mathbf{r}), \dots, \mathbf{f}_N(\mathbf{r})) \approx \sum_{i=1}^N E_{\text{cell}}([\rho]; \mathbf{f}_i(\mathbf{r})) \quad (25)$$

where $E_{\text{cell}}([\rho]; \mathbf{r}_i)$ is the electrostatic energy of the cell around an electron at position \mathbf{r}_i , equal to the sum of the attraction between the electron and the background contained in the cell and the background–background repulsion inside the cell.⁴

Notice that, for a given SCE configuration, the electrostatic energy $\varepsilon_{\text{es}}(\mathbf{r}, \mathbf{f}_2(\mathbf{r}), \dots, \mathbf{f}_N(\mathbf{r}))$ of eq 25 is equal to $N\tilde{w}_{\infty}(\mathbf{r})$, where $\tilde{w}_{\infty}(\mathbf{r})$ is given in eq 23. The PC model is then trying to approximate $N\tilde{w}_{\infty}(\mathbf{r})$ by constructing the electrostatic energy $E_{\text{cell}}([\rho]; \mathbf{r}_i)$ of a cell around the electron at position \mathbf{r}_i . However, and this is a crucial step to understand the gauge of the PC model, once an approximation for $E_{\text{cell}}([\rho]; \mathbf{r}_i)$ has been built, the sum over the N electrons on the right-hand side of eq 25 is replaced by $NE_{\text{cell}}([\rho]; \mathbf{r})$.⁴ In the original derivation of the PC model,⁴ this step was seen as a further approximation. From the derivation of eqs 17–21, we see that this is not an approximation but an exact feature of the $\lambda \rightarrow \infty$ limit, summarized in eq 24. Because of this transformation, the local electrostatic energy that the PC model is trying to approximate is then exactly the same as that of the exchange-correlation hole of eq 21.

It is important to stress that the PC cell is *not* an approximation to the exchange-correlation hole in the $\lambda \rightarrow \infty$ limit.⁴ However, its electrostatic energy (electron–background attraction plus background–background repulsion) is an approximation to the electrostatic potential of the exchange correlation hole, eq 11. This concept is further clarified in the Appendix, where the case of the uniform electron gas at extreme low density is treated explicitly.

The simplest approximation to the PC cell is a sphere of uniform density $\rho(\mathbf{r})$ around the electron at position \mathbf{r} with a radius $r_s(\mathbf{r}) = (4\pi/3\rho(\mathbf{r}))^{-1/3}$ fixed by the condition that the fictitious positive background exactly neutralizes the electron at its center. This leads to the simple PC-LDA approximation⁴

$$w_{\text{PC}}^{\text{LDA}}(\mathbf{r}) = -\frac{9}{10} \left(\frac{4\pi}{3} \right)^{1/3} \rho(\mathbf{r})^{1/3} \quad (26)$$

If we approximate the dipole moment of the cell in terms of the gradient of the density and we set it equal to zero, we obtain the PC-GGA expression⁴

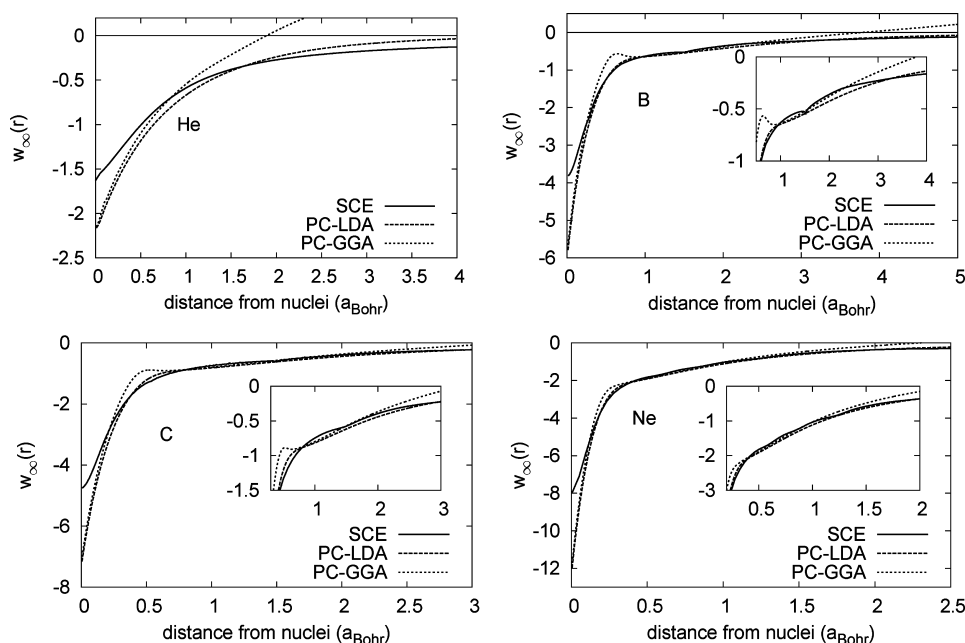


Figure 1. Energy density in the gauge of the electrostatic potential of the exchange-correlation hole, eq 11, in the $\lambda \rightarrow \infty$ limit. The exact SCE result of eq 21 is compared with the PC-LDA and PC-GGA approximations of eqs 26 and 27.

$$w_{\text{PC}}^{\text{GGA}}(\mathbf{r}) = w_{\text{PC}}^{\text{LDA}}(\mathbf{r}) + \frac{3}{350} \left(\frac{3}{4\pi} \right)^{1/3} \frac{|\nabla \rho(\mathbf{r})|^2}{\rho(\mathbf{r})^{7/3}} \quad (27)$$

In Figure 1, we compare the exact $\lambda \rightarrow \infty$ energy densities of eq 21 with the PC-LDA and PC-GGA approximations of eqs 26 and 27 for the He atom, the sphericalized B and C atoms, and the Ne atom, using accurate Hylleras and quantum Monte Carlo densities.^{55–57} We see that the PC model becomes a rather good approximation in the valence region of B, C, and Ne, while being quite poor in the core region, and especially at the nucleus. The PC-LDA energy density is actually a better local approximation than the PC-GGA except close to the nucleus. The PC-GGA performs better globally (see Table 1),

Table 1. Global Value $W_\infty[\rho] = \int \rho(\mathbf{r}) w_\infty[\rho](\mathbf{r}) d\mathbf{r}$ for Small Atoms at Different Levels of Approximation^a

	SCE	PC-LDA	PC-GGA
H [−]	−0.569	−0.664	−0.559
He	−1.498	−1.735	−1.468
Li	−2.596	−2.983	−2.556
Be	−4.021	−4.561	−3.961
B	−5.706	−6.412	−5.650
C	−7.781	−8.650	−7.719
Ne	−19.993	−21.647	−19.999

^aThe SCE corresponds to the exact value, eq 21, while PC-LDA and PC-GGA correspond, respectively, to eqs 26 and 27.

but we clearly see that this is due to an error compensation between the core region and the intershell region. In the tail of the density, the PC-GGA energy density of eq 27 diverges. Notice that the exact SCE energy densities have kinks (clearly visible in the insets of Figure 1), which occur each time we have a configuration with one of the electrons at infinity.

The approximations made in the PC model are (i) neglecting the cell–cell interaction and (ii) the gradient expansion of eqs 26 and 27, which assumes a slowly varying density. At the nucleus, we can easily construct what would be the “exact” PC

cell, so that we can at least remove approximation ii and check the effect of approximation i alone. The “exact” PC cell around the nucleus is the sphere Ω_1 of radius a_1 , with

$$\int_0^{a_1} 4\pi r^2 \rho(r) dr = 1 \quad (28)$$

and the “exact” value of $w_{\text{PC}}(r = 0)$ is

$$\begin{aligned} w_{\text{PC}}(\mathbf{r} = 0) &= - \int_{\Omega_1} d\mathbf{r} \frac{\rho(\mathbf{r})}{r} + \frac{1}{2} \int_{\Omega_1} d\mathbf{r} \int_{\Omega_1} d\mathbf{r}' \frac{\rho(\mathbf{r}) \rho(\mathbf{r}')}{|\mathbf{r} - \mathbf{r}'|} \end{aligned} \quad (29)$$

In Table 2, we compare the values at the nucleus from the exact SCE, the PC-LDA or PC-GGA (they become equal at the nucleus), and the result of eq 29 for several atoms. We see that eq 29 is very accurate for $N = 2$: in this case, in fact, when the reference electron is at the nucleus, the other one is at infinity, so that the cell–cell interaction becomes indeed zero. For $N >$

Table 2. Comparison of the Values at the Nucleus of the Energy Density in the Gauge of the Exchange-Correlation Hole Potential in the Strong-Interaction Limit for Small Atoms^a

	$w_{\text{SCE}}(r = 0)$	$w_{\text{PC}}^{\text{GGA}}(r = 0)$	$w_{\text{PC}}(r = 0)$
H [−]	−0.6825	−0.9671	−0.7157
He	−1.6883	−2.1729	−1.6672
Li	−2.2041	−3.4019	−2.6396
Be	−3.1568	−4.6578	−3.6354
B	−3.8230	−5.8995	−4.6190
C	−4.7727	−7.1446	−5.6050
Ne	−8.0276	−12.119	−9.5463

^aThe value $w_{\text{SCE}}(r = 0)$ corresponds to the exact expression of eq 21. The value $w_{\text{PC}}^{\text{GGA}}(r = 0)$ is the PC gradient expansion approximation of eqs 26 and 27 (the PC-LDA and PC-GGA are equal at the nucleus), and $w_{\text{PC}}(r = 0)$ is the value from the “exact” PC cell of eq 29.

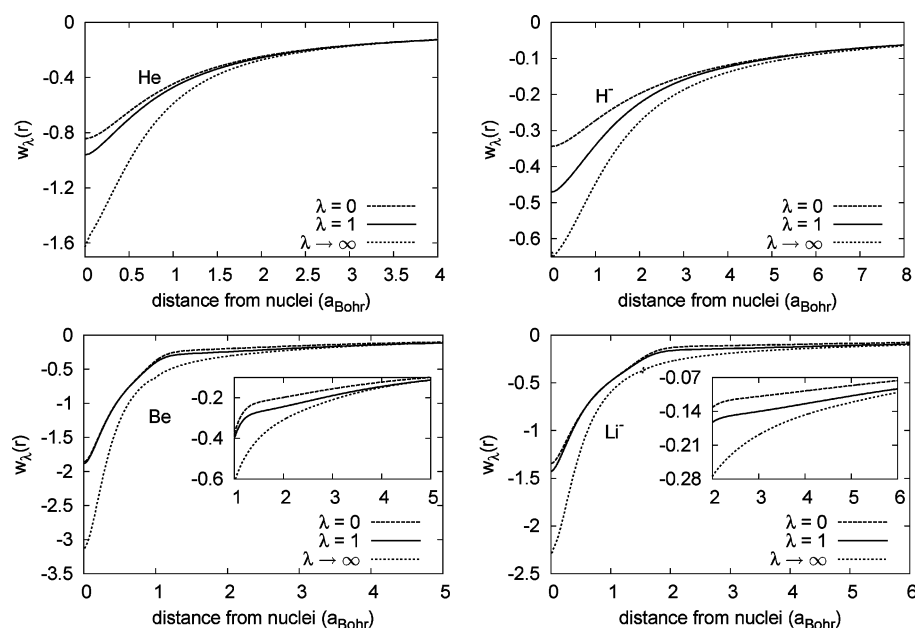


Figure 2. Energy densities in the gauge of the electrostatic potential of the exchange-correlation hole for accurate full-CI densities (aug-cc-pVTZ) and coupling strength $\lambda = 0, 1$ and ∞ .

2, we see that the “smearing hypothesis,” i.e., the idea that the cell–cell interaction is negligible, leads to some errors, although there is an improvement with respect to the gradient expansion of eqs 26 and 27, reducing the relative error of about a factor 2. Along these lines, one might try to construct an improved PC model that performs locally better than the PC-GGA, which, as we have shown, achieves good global accuracy at the price of error compensation between different regions of space.

5. ENERGY DENSITIES ALONG THE ADIABATIC CONNECTION

5.1. Kohn–Sham ($\lambda = 0$). At zero coupling strength, the exact solution for the wave function Ψ_0 becomes a Slater determinant $\Phi = |\phi_1 \dots \phi_N\rangle$, and the energy density $w_0[\rho](\mathbf{r})$ in the gauge of the exchange-correlation hole is given by the electrostatic potential of the KS exchange hole $h_x(\mathbf{r}, \mathbf{r}')$:

$$w_0[\rho](\mathbf{r}) = \frac{1}{2} \int \frac{h_x(\mathbf{r}, \mathbf{r}')}{|\mathbf{r} - \mathbf{r}'|} d\mathbf{r}' \quad (30)$$

as the pair density simply writes

$$P_2^0(\mathbf{r}, \mathbf{r}') = \rho(\mathbf{r}) \rho(\mathbf{r}') + \rho(\mathbf{r}) h_x(\mathbf{r}, \mathbf{r}') \quad (31)$$

In eq 30, one can use the exact exchange hole built from a Hartree–Fock like expression in terms of the KS orbitals ϕ_i or a density functional approximation for $h_x(\mathbf{r}, \mathbf{r}')$, e.g., the one of Becke and Roussel.⁵⁸ These two choices would correspond, respectively, to construct a hyper-GGA and a meta-GGA functional from a local interpolation along the adiabatic connection.

The aim of the present work is a preliminary study of *exact* energy densities along the adiabatic connection. The exact KS orbitals and the corresponding noninteracting potential \hat{V}_{ext}^0 for a given physical density can be found accurately, e.g., by inversion of the KS equations^{59–64} or by the use of Lieb’s Legendre transform DFT formalism.^{34,65,66}

For an ISI-like interpolation on the energy density, $w_0[\rho](\mathbf{r})$ will be a key ingredient. Additionally, knowledge of the next leading order in the asymptotic expansion of the local energy

density around $\lambda = 0$ is necessary, but not available yet. The next leading order in the asymptotic expansion constitutes an active field of research in our group (see also the discussion in section 7).

5.2. Physical ($\lambda = 1$). To compute the exact energy density at coupling-strength $\lambda = 1$, we resort to

$$w_1[\rho](\mathbf{r}) = \frac{1}{2\rho(\mathbf{r})} \int \frac{P_2^1(\mathbf{r}, \mathbf{r}')}{|\mathbf{r} - \mathbf{r}'|} d\mathbf{r}' - \frac{1}{2} \int \frac{\rho(\mathbf{r}')}{|\mathbf{r} - \mathbf{r}'|} d\mathbf{r}' \quad (32)$$

with the pair density given by the full many-body wave function Ψ_1 in eq 13. The density $\rho_1(\mathbf{r})$ corresponding to $P_2^1(\mathbf{r}, \mathbf{r}')$ defines the density $\rho(\mathbf{r}) = \rho_1(\mathbf{r})$ to be held constant along the adiabatic connection.

The exact $w_1[\rho](\mathbf{r})$ can serve as benchmark for models on $w_\lambda[\rho](\mathbf{r})$ but also gives an estimate of the importance of the strong-interaction limit in the $w_\lambda[\rho](\mathbf{r})$ model. If the physical system is close to the KS one, correlation is less important and already Hartree–Fock should perform well. In this case, we expect that inclusion of the $\lambda \rightarrow \infty$ information in the $w_\lambda[\rho](\mathbf{r})$ model will not lead to a major improvement. In contrast, for more strongly correlated systems the physical energy density should tend more toward the $\lambda \rightarrow \infty$ limit and the SCE functional can provide useful input for an accurate model for $w_\lambda[\rho](\mathbf{r})$. The relevance of the strong-interaction limit will be discussed in the next section.

5.3. Results. 5.3.1. Coulomb External Potential. We have performed full-CI calculations in an aug-cc-pVTZ basis for some two and four electron atoms within the Gamess-US package⁶⁷ to obtain an accurate ground state wave function for the physical interaction strength. Starting from this, we are able to calculate the energy density in the gauge of the exchange-correlation hole for $\lambda = 0, 1, \infty$.

At $\lambda = 1$, we calculate the energy density from the full-CI pair density, eq 32, with a program similar to the one used for the calculation of v_{cond} in ref 52.

For the energy density at $\lambda = 0$, eq 30, we have to compute the single particle KS orbitals corresponding to the full-CI

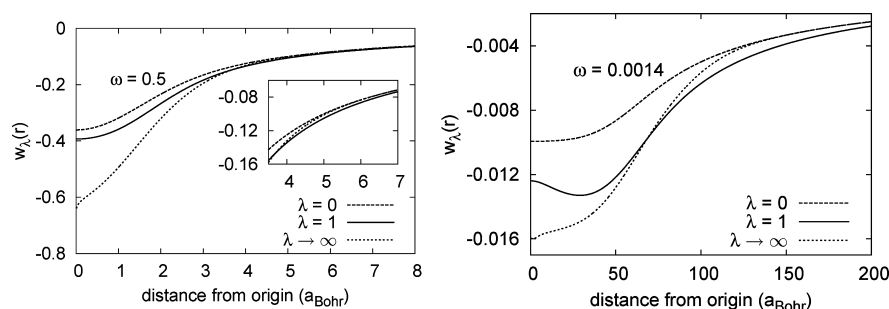


Figure 3. Energy densities in the gauge of the electrostatic potential of the exchange-correlation hole for Hooke's atoms with less pronounced correlation ($\omega = 0.5$) and pronounced correlation ($\omega = 0.0014$).

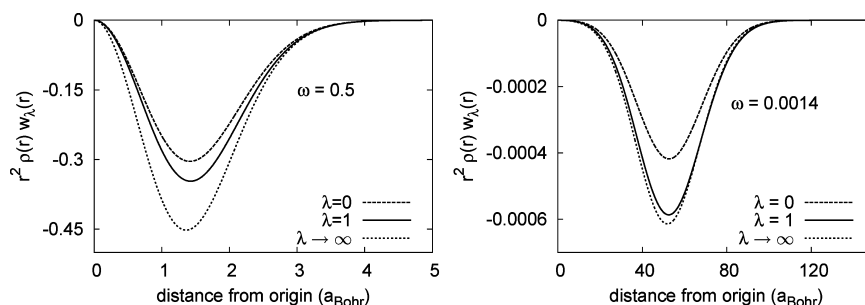


Figure 4. The same energy densities of Figure 3 multiplied by the density.

density first. In the case of two electron atoms, they are readily constructed by the simple relation

$$\phi(\mathbf{r}) = \sqrt{\frac{\rho(\mathbf{r})}{2}} \quad (33)$$

For the four electron atoms, we choose the scheme of van Leeuwen et al.^{60,61} to invert the KS equations. In the strong-interaction limit, we calculate the energy density within the SCE concept, see section 4.1 and refs 8 and 9.

In Figure 2, we show the energy densities for $\lambda = 0, 1, \infty$ for two- and four-electron atoms. As expected, He and Be are relatively weakly correlated, and their $\lambda = 1$ energy densities are much closer to the KS ones than to the SCE ones. Here, a description at the Hartree–Fock level is very reasonable and gives indeed at least 98.5% of the total energy. The anion H^- , instead, being a system with a more diffuse density and thus more correlated, has a physical energy density that is much more in between the KS and the SCE curves, with a Hartree–Fock treatment giving only 94% of the total energy. Here, we expect the inclusion of the information from the strong-interaction limit to be important. The valence regions of Be and Li^- (see the insets in Figure 2) can also be better described by a proper inclusion of the $\lambda = \infty$ information.

5.3.2. Harmonic External Potential. Another useful class of systems for investigation of the impact of the strong-interaction limit on the physical energy density is given by 3D model quantum dots, also known as Hooke's atoms. Here, two electrons (still interacting with the $1/r$ Coulomb repulsion) are confined in the harmonic external potential, and correlation gains importance as the spring constant of the harmonic potential is lowered. We have computed the energy density for Hooke's atoms with spring constants for which the analytic solution for the wave function can be found.⁶⁸ The results are displayed in Figures 3 and 4 for the largest and smallest spring constant considered. As expected, the physical energy density comes closer to the SCE energy density in the more strongly

correlated case. Additionally, as a remarkable feature, we observe that the physical energy density crosses the SCE energy density. Intuitively, one would expect the physical energy density to be always in between the KS and SCE energy densities, as the KS energy density represents the weakest possible correlation and the SCE energy density the strongest possible correlation in the given density. However, the wave functions are chosen according to the global quantities

$$\min_{\Psi \rightarrow \rho} \langle \Psi | \hat{T} | \Psi \rangle \Rightarrow \Psi_{\text{KS}} \quad (34)$$

$$\min_{\Psi \rightarrow \rho} \langle \Psi | \hat{V}_{\text{ee}} | \Psi \rangle \Rightarrow \Psi_{\text{SCE}} \quad (35)$$

$$\min_{\Psi \rightarrow \rho} \langle \Psi | \hat{T} + \hat{V}_{\text{ee}} | \Psi \rangle \Rightarrow \Psi_{\lambda=1} \quad (36)$$

yielding the global inequalities

$$\langle \Psi_{\text{SCE}} | \hat{V}_{\text{ee}} | \Psi_{\text{SCE}} \rangle \leq \langle \Psi_{\lambda=1} | \hat{V}_{\text{ee}} | \Psi_{\lambda=1} \rangle \leq \langle \Psi_{\text{KS}} | \hat{V}_{\text{ee}} | \Psi_{\text{KS}} \rangle \quad (37)$$

Locally, these inequalities can be violated without violating the global ones, and hence the physical energy density can go below the SCE energy density.

The crossing feature can be attributed to “polarization” effects between the two electrons, reflected in the pair density. Here, by “polarization” we mean a two-body effect, i.e., how the position of one electron is influenced by the other.⁶⁹ When one of the electrons is at infinity, the other electron will be mainly found around the origin (where the minimum of the external potential is located). The physical ($\lambda = 1$) description of this electron is then a charge distribution around the origin. As the other electron approaches the origin from infinity, this charge distribution is deformed. For the KS ($\lambda = 0$) system, where we have an independent-electrons picture, this effect is not contained in the pair density as it would be expressed by a term of mutual dependence between the positions of the electrons that cannot arise when we use one-particle orbitals to

construct the wave function. For the SCE system ($\lambda = \infty$) there is a *perfect* mutual dependence between the two electronic positions, with zero kinetic energy. In other words, the electrons are modeled as point charges and not as charge distributions. The proper description of the “polarization” effect is thus missing in the SCE wave function and can probably be recovered, at least partially, by considering the next leading term in the $\lambda \rightarrow \infty$ expansion, corresponding to zero-point oscillations around the SCE solution.⁹

To underline this argument, we have computed the asymptotic behavior of the physical energy density for the Hooke’s atom with $\omega = 0.5$ using the asymptotic expansion of the physical pair density⁶⁹

$$\frac{P(\mathbf{r}, \mathbf{r}')}{\rho(\mathbf{r})\rho_{N-1}(\mathbf{r}')} \rightarrow 1 - 2\frac{r'}{r} \cos(\Delta\Omega) + \dots \quad (r \rightarrow \infty) \quad (38)$$

where $\rho_{N-1}(\mathbf{r}')$ is the density of the $(N - 1)$ -particle system and $\Delta\Omega$ the angle between \mathbf{r} and \mathbf{r}' . The second order term in eq 38 represents the mentioned “polarization” correction. As can be seen from Figure 5, for large $|\mathbf{r} - \mathbf{r}'|$ the energy density in

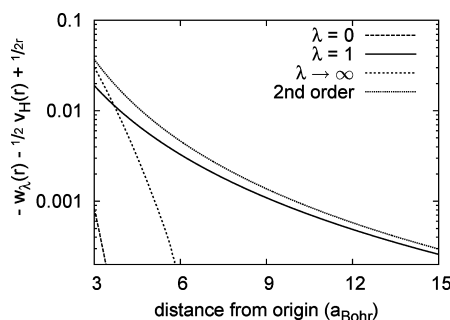


Figure 5. Difference between the energy density and the first order correction of eq 38, including the Hartree contribution $1/2v_H(\mathbf{r})$ (total pair density) for the Hooke’s atom with $\omega = 0.5$. The energy densities are in the gauge of the electrostatic potential of the exchange-correlation hole and are computed from the KS, physical, and SCE pair density and are compared with the correction from the second term in the asymptotic expansion of the physical pair density, eq 38.

the KS and SCE case behaves like $-1/2r$, which corresponds to the first order in the expansion of the physical pair density. Inclusion of the second order term in the energy density gives essentially the physical behavior and deviates from the KS and SCE energy densities.

Although the crossing happens in a region in which the density is very small and thus with an almost negligible energetic contribution (see Figure 4 for the energetically meaningful product of w_λ times the density), the analysis presented here can be helpful in constructing models for $w_\lambda[\rho](\mathbf{r})$. Notice that, instead, with the Coulomb external potential we always observed, so far, the expected behavior $w_{\lambda \rightarrow \infty}(\mathbf{r}) \leq w_{\lambda=1}(\mathbf{r}) \leq w_{\lambda=0}(\mathbf{r})$ everywhere.

6. THE LOCAL FORM OF THE LIEB–OXFORD BOUND

The Lieb–Oxford (LO) bound^{22–24} is a rigorous lower bound to the indirect part of the electron–electron repulsion energy $\tilde{W}[\Psi]$ associated with a given many-electron wave function Ψ :

$$\tilde{W}[\Psi] \equiv \langle \Psi | \hat{V}_{ee} | \Psi \rangle - U[\rho_\Psi] \geq -C \int d\mathbf{r} \rho_\Psi(\mathbf{r})^{4/3} \quad (39)$$

where $\rho_\Psi(\mathbf{r})$ is the density obtained from the wave function Ψ . The positive constant C is rigorously known to have a value^{23,24} $C \leq 1.679$. It has been suggested^{70–72} that a tighter bound can be obtained by taking the value of C that corresponds to the low-density limit of the uniform electron gas, $C \approx 1.44$, since the bound is known to be more challenged when the number of electrons increases²³ and when the system has low density.⁷³

The LO bound translates into a lower bound for the exchange and exchange-correlation functionals:^{70,73}

$$E_x[\rho] \geq E_{xc}[\rho] \geq -C \int d\mathbf{r} \rho(\mathbf{r})^{4/3} \quad (40)$$

simply because $E_x[\rho] = W_{\lambda=0}[\rho]$ is the indirect Coulomb repulsion of the Slater determinant of KS orbitals, and $E_{xc}[\rho]$ is the sum of the indirect Coulomb repulsion of the physical wave function, $W_{\lambda=1}[\rho]$, plus the correlation correction to the kinetic energy, which is always positive.

The way the LO bound is used in the construction of approximate functionals is, usually (with the exception of ref 74), by imposing it locally (see, e.g., refs 25 and 27). That is, a given approximate exchange-correlation functional, $E_{xc}^{DFA}[\rho] = \int d\mathbf{r} \rho(\mathbf{r}) \varepsilon_{xc}^{DFA}(\mathbf{r})$, is required to satisfy

$$\varepsilon_{xc}^{DFA}(\mathbf{r}) \geq -C\rho(\mathbf{r})^{1/3} \quad (41)$$

This is a sufficient condition to ensure the global bound of eq 40, but it is by no means necessary (see, e.g., ref 75). In other words, there is no proof that a local version of the LO bound should hold. Actually, before even asking whether a local version of the LO bound does hold or not, we need to understand to which definition (gauge) of the energy density the local LO bound of eq 41 applies. In fact, since energy densities are not uniquely defined, the inequality 41 should be satisfied only for a well-defined gauge: one can indeed always add to $\varepsilon_{xc}^{DFA}(\mathbf{r})$ a quantity that integrates to zero and violates eq 41 in some region of space.

We argue here that (i) the gauge of the local LO bound is the conventional one of the electrostatic energy of the exchange-correlation hole and (ii) the local LO bound is then certainly violated, at least in the tail region of an atom or of a molecule, and in the bonding region of a stretched molecule. The argument behind point i is the following. For a given density ρ , the wave function $\Psi[\rho]$ that maximally challenges¹¹ the LO bound is the one that minimizes the expectation $\langle \Psi[\rho] | \hat{V}_{ee} | \Psi[\rho] \rangle$, i.e., by definition, $\Psi_{SCE}[\rho]$. In fact, we also have

$$E_x[\rho] \geq E_{xc}[\rho] \geq W_\infty[\rho] \geq -C \int d\mathbf{r} \rho(\mathbf{r})^{4/3} \quad (42)$$

In section 4, we have discussed the energy density associated with $W_\infty[\rho]$ in the gauge of the electrostatic potential of the exchange-correlation hole. We have also shown that this energy density can be approximated by the PC model that considers the electrostatic energy of a cell around the reference electron of positive charge $\rho_+(\mathbf{r}) = \rho(\mathbf{r})$. The LDA version of this approximation has exactly the same form of the local LO bound. Moreover, the recently suggested value⁷¹ $C \approx 1.44$ is extremely close to the one of the PC-LDA model, $C_{PC} \approx 1.45$. Notice that the fact that the PC model is in the gauge of the electrostatic energy of the exchange-correlation hole follows from the properties of the strong-interaction limit of DFT, in particular eq 24. If the PC model is an approximation in this gauge, and if the LO bound is locally equal to it, then conclusion i should follow, although this is not a rigorous

argument, but only a plausible one. Another way to arrive at the same conclusion comes from the fact that the local form of the tightened LO bound corresponds to approximate, in each point of space, the exchange-correlation hole with the one of the extremely correlated ($\lambda \rightarrow \infty$) electron gas, as illustrated in the Appendix. This would imply, again, an energy density in the gauge of the exchange-correlation hole.

We then easily see that the local LO bound of eq 41 is certainly violated in the tail region of an atom or a molecule, where the exact energy density in the conventional exchange-correlation hole gauge goes like $-1/(2r)$ while the right-hand side of eq 41 decays exponentially. The local bound is also violated in the bond region of a stretched molecule. As an example, we show in Figure 6 the energy densities of the

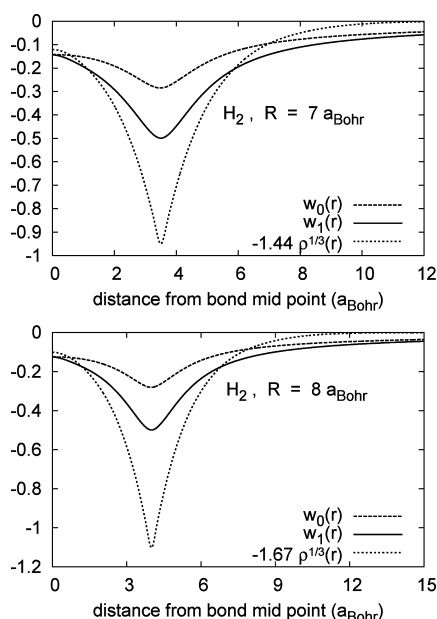


Figure 6. Violation of the local form of the Lieb–Oxford bound for the stretched H_2 molecule.

stretched H_2 molecule for $\lambda = 0$ and $\lambda = 1$: with $C = 1.44$, the local bound is violated in the bond region when the internuclear distance is $R \gtrsim 7$ au and, with $C = 1.67$, when $R \gtrsim 8$ au. Our results also give formal support to the recent work of Vilhena et al.,⁷⁶ who report a detailed investigation of the consequences of the local LO bound on approximate functionals. From their work, we see that for the G2 sets, the violation of the local LO bound happens in energetically unimportant regions. The bonding region of a stretched molecule shown in our Figure 6 is also energetically unimportant. However, the corresponding KS potential in the same region has important features relevant for a proper description of the breaking of the bond,^{52,77} although this is expected to be a very nonlocal effect.

As a concluding remark, we can say that it is very difficult, or maybe even impossible, to find a rigorous local lower bound for the energy density. In fact, we have just seen in section 5 that, at least for the harmonic external potential, it is not even true that $w_{\lambda=1}(\mathbf{r}) \geq w_{\infty}(\mathbf{r})$ everywhere. This means that even if we maximize the correlation between the electrons, we do not construct a rigorous local lower bound, but only a global one.

7. CONCLUSIONS AND PERSPECTIVES

We have derived an exact expression for the energy density in the strong-interaction limit of DFT in the gauge of the exchange-correlation-hole electrostatic potential, and we have computed it for small atoms and model quantum dots. A careful analysis of the point-charge plus continuum (PC) model showed that this approximation is formulated in the same gauge, and a comparison with the exact results showed that it is locally reasonable in the atomic valence region.

Our formalism also strongly suggests that the local version of the Lieb–Oxford bound is formulated in the same conventional gauge of the exchange-correlation hole, and it is then certainly violated. Our findings are in agreement with (and give formal support to) the very recent results of Vilhena et al.⁷⁶ (which only appeared when this manuscript was completed). More generally, our results suggest that it is very difficult (if not impossible) to derive a rigorous local lower bound for the energy density.

We have also discussed the idea of a local interpolation along the adiabatic connection. The values of the local energy density in the same gauge at $\lambda = 0$ and $\lambda = \infty$ are now available, either exactly or in an approximate way. Even if we have found that in the harmonic external potential the physical energy density is not always in between the $\lambda = 0$ and the $\lambda = \infty$ curves, the regions of space in which the expected order is reversed are energetically not important. In the external Coulomb potential, we have found, instead, the expected behavior $w_{\lambda \rightarrow \infty}(\mathbf{r}) \leq w_{\lambda=1}(\mathbf{r}) \leq w_{\lambda=0}(\mathbf{r})$ everywhere.

To really be able to build a local interpolation, at least the slope at $\lambda = 0$ and possibly the next leading term at $\lambda = \infty$ are also needed in a local form, and in the same gauge. A first step toward the construction of a local slope at $\lambda = 0$ is to produce exact results for this quantity, crucial to assessing approximations. This can be achieved with the Legendre transform techniques developed in refs 33 and 34 and is currently being investigated. A possible way, then, to construct an approximate local slope is to use the so-called “extended Overhauser model”^{78–80} locally, in a perturbative way. A local next leading term at $\lambda = \infty$ can also be constructed by deriving the exact exchange-correlation hole corresponding to the wave function of the zero-point oscillations, discussed in ref 9. All of these aspects will be investigated in future works.

■ APPENDIX

A. PC Cell and xc Hole

In this appendix, we clarify the difference between the exchange-correlation hole and the PC cell by considering the uniform electron gas in the extreme low-density limit, further extending the argument already given in the appendix of ref 4.

More than 70 years ago, Wigner^{81,82} pointed out that electrons embedded in a compensating uniformly charged background would crystallize at sufficiently low values of the density ρ . The SCE construction can be seen as nothing else than the Wigner idea generalized to a nonuniform density $\rho(\mathbf{r})$. Indeed, in ref 9 the SCE formalism is presented as a “floating” Wigner crystal in a non-Euclidean space, with the metric determined by the density $\rho(\mathbf{r})$.

In the case of the uniform electron gas, the SCE co-motion functions are simply the positions of the bcc lattice points with the origin fixed at the reference electron. Notice that the constraint that the density is uniform, eq 35, forces us to consider a “floating” Wigner crystal, which corresponds to the

linear superposition of all of the possible origins and orientations of the crystal, thus restoring the translational symmetry. The exchange-correlation hole $\rho(g(r) - 1)$, with $g(r)$ the pair-distribution function, can then be simply constructed by considering that the expected number of electrons in a spherical shell of radius r and thickness dr around the reference electron at the origin is given by

$$dN(r|0) = \rho g(r) 4\pi r^2 dr \quad (43)$$

We can then place very narrow normalized Gaussians (almost δ functions) at the bcc sites around the reference electron and take the spherical average. This way, we obtain the extreme low-density limit of $g(r)$. In Figure 7, we compare this low-

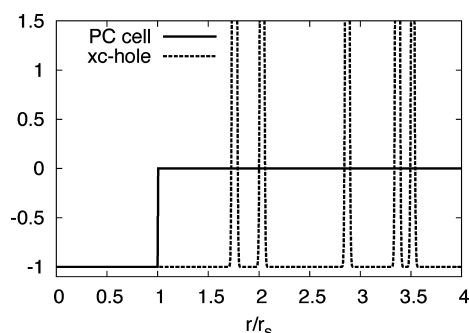


Figure 7. PC cell divided by the density ρ (i.e., $c(r) = -\theta(r_s - r)$) and the pair-correlation function $g(r) - 1$, corresponding to the exchange-correlation hole divided by the density ρ for the extreme low-density electron gas.

density (or SCE) $g(r) - 1$ with the PC cell $c(r)$ in the same units, $c(r) = -\theta(r_s - r)$, with $\theta(x)$ the Heaviside step function. We see that the two are very different, except for $r/r_s \leq 1$. The exchange-correlation hole has positive peaks (indicating the positions of the other electrons) that extend to $r \rightarrow \infty$ (perfect long-range order). Notice that the exchange-correlation hole for the broken symmetry solution (without translational invariance) would be, instead, much less structured, but here we are interested in the solution constrained to the uniform density. The way the electrostatic energy is calculated from the PC cell and the exchange-correlation hole is also different:⁴

$$w = \rho \int \frac{g(r) - 1}{r} dr \quad (44)$$

$$w = -\rho \int \frac{c(r)}{r} dr + \frac{\rho^2}{2} \int dr \int dr' \frac{c(r) c(r')}{|\mathbf{r} - \mathbf{r}'|} \quad (45)$$

When we use the exchange-correlation hole to evaluate the energy, eq 44, we need to evaluate an infinite sum (all the peaks in Figure 7) which converges very badly (the Madelung sum) and that can be dealt with, for example, the Ewald method. When we use the PC cell, instead, we face two very simple, short-ranged integrals.⁵⁴ The two results differ only by 0.45%, as was already noted in ref 83, where it was also proven that the PC value is a rigorous lower bound for the energy of the uniform electron gas.

Notice that if, instead, we consider the PC cell as a model for the exchange correlation hole and we use $c(r)$ in eq 44 instead of $g(r) - 1$, we get a very poor result⁴ with an error of $\sim 17\%$. The PC model does approximate the electrostatic potential of the exchange-correlation hole by constructing it in a different way.

AUTHOR INFORMATION

Corresponding Author

*E-mail: p.gorigiorgi@vu.nl

Notes

The authors declare no competing financial interest.

ACKNOWLEDGMENTS

The authors thank Robert van Leeuwen for sharing the program for the inversion of the KS equations. We are grateful to Oleg Gritsenko for helpful assistance in developing the program for the calculation of the physical energy density, and Andrew Teale for a critical reading of the manuscript. AM acknowledges Evert Jan Baerends for his warm hospitality at the Postech University in Pohang, Korea, where part of this work was done. PG-G thanks Gaetano Senatore for useful discussions. This work was supported by The Netherlands Organization for Scientific Research (NWO) through a Vidi grant.

REFERENCES

- (1) Cohen, A. J.; Mori-Sánchez, P.; Yang, W. *Chem. Rev.* **2012**, *112*, 289.
- (2) Seidl, M. *Phys. Rev. A* **1999**, *60*, 4387.
- (3) Seidl, M.; Perdew, J. P.; Levy, M. *Phys. Rev. A* **1999**, *59*, 51.
- (4) Seidl, M.; Perdew, J. P.; Kurth, S. *Phys. Rev. A* **2000**, *62*, 012502.
- (5) Seidl, M.; Perdew, J. P.; Kurth, S. *Phys. Rev. Lett.* **2000**, *84*, 5070.
- (6) Gori-Giorgi, P.; Seidl, M.; Vignale, G. *Phys. Rev. Lett.* **2009**, *103*, 166402.
- (7) Gori-Giorgi, P.; Seidl, M. *Phys. Chem. Chem. Phys.* **2010**, *12*, 14405.
- (8) Seidl, M.; Gori-Giorgi, P.; Savin, A. *Phys. Rev. A* **2007**, *75*, 042511.
- (9) Gori-Giorgi, P.; Vignale, G.; Seidl, M. *J. Chem. Theory Comput.* **2009**, *5*, 743.
- (10) Buttazzo, G.; De Pascale, L.; Gori-Giorgi, P. *Phys. Rev. A* **2012**, *85*, 062502.
- (11) Räsänen, E.; Seidl, M.; Gori-Giorgi, P. *Phys. Rev. B* **2011**, *83*, 195111.
- (12) Becke, A. D. *J. Chem. Phys.* **2005**, *122*, 064101.
- (13) Becke, A. D.; Johnson, E. R. *J. Chem. Phys.* **2007**, *127*, 124108.
- (14) Perdew, J. P.; Staroverov, V. N.; Tao, J.; Scuseria, G. E. *Phys. Rev. A* **2008**, *78*, 052513.
- (15) Gori-Giorgi, P.; Savin, A. *J. Phys.: Conf. Ser.* **2008**, *117*, 012017.
- (16) Savin, A. *Chem. Phys.* **2009**, *356*, 91.
- (17) Burke, K.; Cruz, F. G.; Lam, K.-C. *J. Chem. Phys.* **1998**, *109*, 8161.
- (18) Cohen, L. *J. Chem. Phys.* **1979**, *70*, 788.
- (19) Cohen, L. *J. Chem. Phys.* **1996**, *80*, 4277.
- (20) Cohen, L. *Phys. Lett. A* **1996**, *212*, 315.
- (21) Ayers, P.; Parr, R. G.; Nagy, A. *Int. J. Quantum Chem.* **2002**, *90*, 309.
- (22) Lieb, E. H. *Phys. Lett.* **1979**, *70A*, 444.
- (23) Lieb, E. H.; Oxford, S. *Int. J. Quantum Chem.* **1981**, *19*, 427.
- (24) Chan, G. K.-L.; Handy, N. C. *Phys. Rev. A* **1999**, *59*, 3075.
- (25) Perdew, J. P.; Burke, K.; Ernzerhof, M. *Phys. Rev. Lett.* **1996**, *77*, 3865.
- (26) Tao, J.; Perdew, J. P.; Staroverov, V. N.; Scuseria, G. E. *Phys. Rev. Lett.* **2003**, *91*, 146401.
- (27) Haunschild, R.; Odashima, M. M.; Scuseria, G. E.; Perdew, J. P.; Capelle, K. *J. Chem. Phys.* **2012**, *136*, 184102.
- (28) Harris, J.; Jones, R. J. *Phys. F* **1974**, *4*, 1170.
- (29) Langreth, D. C.; Perdew, J. P. *Solid State Commun.* **1975**, *17*, 1425.
- (30) Gunnarsson, O.; Lundqvist, B. I. *Phys. Rev. B* **1976**, *13*, 4274.
- (31) Kohn, W.; Sham, L. J. *Phys. Rev. A* **1965**, *140*, 1133.
- (32) Görling, A.; Levy, M. *Phys. Rev. B* **1993**, *47*, 13105.

- (33) Teale, A. M.; Coriani, S.; Helgaker, T. *J. Chem. Phys.* **2009**, *130*, 104111.
- (34) Teale, A. M.; Coriani, S.; Helgaker, T. *J. Chem. Phys.* **2010**, *132*, 164115.
- (35) Becke, A. D. *J. Chem. Phys.* **1993**, *98*, 1372.
- (36) Becke, A. D. *J. Chem. Phys.* **1993**, *98*, 5648.
- (37) Stephens, P. J.; Devlin, F. J.; Chabalowski, C. F.; Frisch, M. J. *J. Phys. Chem.* **1994**, *98*, 11623.
- (38) Lee, C.; Yang, W.; Parr, R. G. *Phys. Rev. B* **1988**, *37*, 785.
- (39) Vosko, S. J.; Wilk, L.; Nusair, M. *Can. J. Phys.* **1980**, *58*, 1200.
- (40) Burke, K.; Ernzerhof, M.; Perdew, J. P. *Chem. Phys. Lett.* **1997**, *265*, 115.
- (41) Ernzerhof, M. *Chem. Phys. Lett.* **1996**, *263*, 499.
- (42) Mori-Sanchez, P.; Cohen, A. J.; Yang, W. T. *J. Chem. Phys.* **2006**, *124*, 091102.
- (43) Peach, M. J. G.; Teale, A. M.; Tozer, D. J. *J. Chem. Phys.* **2007**, *126*, 244104.
- (44) Grimme, S. *J. Chem. Phys.* **2006**, *124*, 034108.
- (45) Sharkas, K.; Toulouse, J.; Savin, A. *J. Chem. Phys.* **2011**, *134*, 064113.
- (46) Brémond, E.; Adamo, C. *J. Chem. Phys.* **2011**, *135*, 024106.
- (47) Toulouse, J.; Sharkas, K.; Brémond, E.; Adamo, C. *J. Chem. Phys.* **2011**, *135*, 101102.
- (48) Yang, W.; Zhang, Y.; Ayers, P. W. *Phys. Rev. Lett.* **2000**, *84*, 5172.
- (49) Cohen, A. J.; Mori-Sanchez, P.; Yang, W. T. *Science* **2008**, *321*, 792.
- (50) Cohen, A. J.; Mori-Sanchez, P.; Yang, W. T. *J. Chem. Phys.* **2008**, *129*, 121104.
- (51) Ayers, P. W. *J. Math. Chem.* **2008**, *43*, 285.
- (52) Buijse, M. A.; Baerends, E. J.; Snijders, J. G. *Phys. Rev. A* **1989**, *40*, 4190.
- (53) Becke, A. *Abstr. Pap.—Am. Chem. Soci.* **2011**, 242.
- (54) Onsager, L. *J. Phys. Chem.* **1939**, *43*, 189.
- (55) Freund, D. E.; Huxtable, B. D.; Morgan, J. D. *Phys. Rev. A* **1984**, *29*, 980.
- (56) Al-Sharif, A. I.; Resta, R.; Umrigar, C. J. *Phys. Rev. A* **1998**, *57*, 2466.
- (57) Toulouse, J. Private communication. The sphericalized densities of the B and C atoms were obtained from variational Monte Carlo using accurate optimized wavefunctions as described in refs 84 and 85.
- (58) Becke, A. D.; Roussel, M. R. *Phys. Rev. A* **1989**, *39*, 3761.
- (59) Wang, Y.; Parr, R. G. *Phys. Rev. A* **1993**, *47*, 1591.
- (60) van Leeuwen, R.; Baerends, E. J. *Phys. Rev. A* **1994**, *49*, 2421.
- (61) Gritsenko, O. V.; van Leeuwen, R.; Baerends, E. J. *Phys. Rev. A* **1995**, *52*, 1870.
- (62) Peirs, K.; Neck, D. V.; Waroquier, M. *Phys. Rev. A* **2003**, *67*, 012505.
- (63) Kadantsev, E. S.; Scott, M. J. *Phys. Rev. A* **2004**, *69*, 012502.
- (64) Astala, R.; Scott, M. J. *Phys. Rev. B* **2006**, *73*, 115127.
- (65) Lieb, E. H. *Int. J. Quantum Chem.* **1983**, *24*, 24.
- (66) Colonna, F.; Savin, A. *J. Chem. Phys.* **1999**, *110*, 2828.
- (67) Schmidt, M. W.; Baldridge, K. K.; Boatz, J. A.; Elbert, S. T.; Gordon, M. S.; Jensen, J. J.; Koseki, S.; Matsunaga, N.; Nguyen, K. A.; Su, S.; Windus, T. L.; Dupuis, M.; Montgomery, J. A. *J. Comput. Chem.* **1993**, *14*, 1347.
- (68) Taut, M. *Phys. Rev. A* **1993**, *48*, 3561.
- (69) Ernzerhof, M.; Burke, K.; Perdew, J. P. *J. Chem. Phys.* **1996**, *105*, 2798.
- (70) Perdew, J. P. In *Electronic Structure of Solids '91*; Ziesche, P., Eschrig, H., Eds.; Akademie Verlag: Berlin, 1991.
- (71) Räsänen, E.; Pittalis, S.; Capelle, K.; Proetto, C. R. *Phys. Rev. Lett.* **2009**, *102*, 206406.
- (72) Odashima, M. M.; Capelle, K. *J. Chem. Phys.* **2007**, *127*, 05416.
- (73) Levy, M.; Perdew, J. P. *Phys. Rev. B* **1993**, *48*, 11638.
- (74) Odashima, M. M.; Capelle, K. *Phys. Rev. A* **2009**, *79*, 062515.
- (75) Zhang, Y.; Yang, W. *Phys. Rev. Lett.* **1998**, *80*, 890.
- (76) Vilhena, J. G.; Räsänen, E.; Lehtovaara, L.; Marques, M. A. L. *Phys. Rev. A* **2012**, *85*, 052514.
- (77) Helbig, N.; Tokatly, I. V.; Rubio, A. *J. Chem. Phys.* **2009**, *131*, 224105.
- (78) Gori-Giorgi, P.; Perdew, J. P. *Phys. Rev. B* **2001**, *64*, 155102.
- (79) Davoudi, B.; Polini, M.; Asgari, R.; Tosi, M. P. *Phys. Rev. B* **2002**, *66*, 075110.
- (80) Gori-Giorgi, P.; Savin, A. *Phys. Rev. A* **2005**, *71*, 032513.
- (81) Wigner, E. P. *Phys. Rev.* **1934**, *46*, 1002.
- (82) Wigner, E. P. *Trans. Faraday Soc.* **1938**, *34*, 678.
- (83) Lieb, E. H.; Narnhofer, H. *J. Stat. Phys.* **1975**, *12*, 291.
- (84) Toulouse, J.; Umrigar, C. J. *J. Chem. Phys.* **2007**, *126*, 084102.
- (85) Umrigar, C. J.; Toulouse, J.; Filippi, C.; Sorella, S.; Hennig, R. G. *Phys. Rev. Lett.* **2007**, *98*, 110201.